Numerical Investigation of a Regenerative Thermal Oxidizer for the Abatement of VOCs

Giuntini Lorenzo[1], Bertei Antonio[*,1], Tortorelli Sonia[1], Percivale Matteo[2], Paoletti Emiliano[2], Tognotti Leonardo[1], Nicolella Cristiano[1], Galletti Chiara[1]

[1]Dipartimento di Ingegneria Civile e Industriale, University of Pisa, Pisa, Italy
[2]Raft s.r.l., Florence, Italy

Abstract
Regenerative Thermal Oxidizers (RTOs) represent a widely accepted technology for the abatement of VOCs, combining high removal efficiency with low operating costs. This work describes a numerical approach for the effective design of an industrial-scale 3-canisters RTOs, coupling a 1-dimensional dynamic model with 3-dimensional CFD simulations. Such a model is validated by using data on pressure drops available from the plant. The model provides a detailed analysis of the thermo-fluid dynamics field at distinct instants within the RTO operation, allowing to explain how different inlet-outlet-purge configurations affect the efficiency of VOCs oxidation.

1. Introduction

VOCs are harmful for human beings and environment and their emissions in the atmosphere must be controlled. For this purpose, thermal oxidizers are commonly used in industry to remove VOCs from gaseous effluents with large volumetric flow rates. The equipment can have high operating costs, as an auxiliary fuel is usually needed to increase the temperature of the polluted stream, so to ensure oxidation of VOCs. However, fuel consumptions can be reduced by preheating the inlet stream with some heat of the exhaust gas [1]. In this framework, Regenerative Thermal Oxidizers (RTOs) represent one of the most effective industrial solutions, as they can provide high efficiencies both in terms of VOCs destruction and heat recovery. RTOs operate in a cyclic manner and are able to efficiently store sensible heat from the outgoing combustion products by employing ceramic masses [2] [3] [4].
RTOs are usually designed with 2 or 3 canisters, which are filled with ceramic beds. An example of a 3-canisters RTO and its configurations are shown in Figure 1. As we can see in Figure 1b, the gaseous effluent first passes through the inlet canister (orange arrows), where it absorbs heat from the ceramic media, hence cooling the media; then, it enters the combustion chamber, where it reaches its ignition point and VOCs destruction takes place, eventually introducing an auxiliary fuel. Exiting from the combustion chamber, the clean hot flue gas flows downward through the outlet canister (blue arrows, about 95% of the total flow rate) and the purge canister (green arrows, about 5% of the total flow rate): here, the heat produced from the combustion of both VOCs and auxiliary fuel is recovered by the ceramic masses, hence preheating the media for the next cycle. To continuously regenerate the heat stored within the ceramic media, and to keep high the heat recovery efficiency, a switching valves system periodically shifts the air flow direction between the canisters. In a 3-canisters RTO, this periodical sequence consists of three alternating configurations as depicted in Figure 1b; at the switching time, the canister serving as inlet turns into a purge canister; in this way the polluted gases that are located there carrying VOCs that have not been yet oxidized, are recycled back to the inlet stream, thus avoiding the presence of VOCs at the chimney. In addition, at the switching of the valves the outlet canister becomes an inlet canister, while the purge canister will act as an outlet canister.

(a)

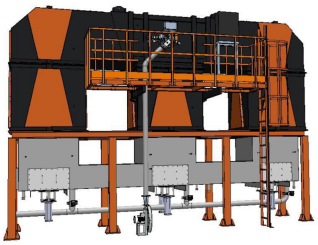

(b)

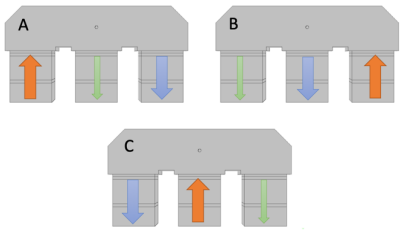

Figure 1. Scheme of: (a) the RTO and (b) its configurations.

In the existing literature, there has been an increasing interest in the development of numerical tools to support the design and optimization of RTOs, as so far no established design procedures are available. Amelio and Morrone [4] as well as Frigerio et al. [5], developed a 1-D model, resolving transient heat balances in the gas and

* Corresponding author antonio.bertei@unipi.it

Deleted: : c.author@myadress.com

solid phases along the axial direction of gas flow, collecting information on pressure drops and energetic performances of different kind of ceramic packings. Recently, Marin et al. [2] summarized the 1-D model equations including reaction and species conservation, in addition to heat balances.

More complex models, based on Computational Fluid Dynamics (CFD) techniques, have been also developed to assist the design and optimization of RTOs. The very first work was provided by Choi et al. [6], who developed a CFD model to study the abatement of VOCs in a 3-canisters RTO, by employing a numerical grid made of 14k cells. Hao et al. [7] performed simulations to study the flow distribution and uniformity inside the ceramic media, assuming them to provide a uniform heat sources. Gosiewski et al. [8] analysed a pilot-scale 2-canister RTO through CFD techniques to get information on flow distribution and pressure drops.

In a recent work [9] we proposed a novel methodology to model an industrial-scale RTO based on a 3-canisters design. The model solves 1-dimensional (1-D) dynamic equations describing the energy conservation in both gas and solid phases, to derive information on the temporal variation of temperature and heat transfer in the ceramic media. Subsequently, such information at different instants is fed to a CFD 3-D model to gain a full insight on the thermo-chemical behaviour of the combustion chamber, including VOCs abatement. The model is employed in the present work to investigate the most critical conditions in the RTO operation and thus to suggest possible design improvement.

2. RTO

The RTO is fed with a gas flow rate of 21200 Nm^3/h, consisting of 20000 Nm^3/h of fresh feed and 1200 Nm^3/h of clean gas recirculated back from the purge canister. The feed enters the RTO with a temperature of 443 K, and it basically consists in a pollutant laden air stream, with a VOC concentration of 650 mg/Nm^3. The RTO is designed with 3 canisters; each canister has a rectangular cross section and is filled with two ceramic beds. The lower bed has a height of 1.2 m, and it is a structured bed made of monolithic blocks (see Figure 2a); the upper bed has a height of 0.15 m, and it is an unstructured bed filled with 3-inches random saddles (see Figure 2b). The main purpose of the monolithic blocks is to exchange heat with the gas, while the aim of the random packings is to protect the monolithic blocks from a rapid degradation due to flame radiation from the combustion chamber. The combustion chamber has a length of about 9 m and is equipped with a circular burner. Here, the auxialiary fuel, i.e. methane, is fed to heat the incoming gas up to the set-point temperature; to this purpose, a temperature controller regulates the methane flow rate to keep the average temperature at 1123 K. On the bottom of each canister, there are two large and one small nozzles, and depending on the canister operation, one of them is open, while the other two are closed. The large nozzles permit the gas stream to enter or exit the RTO, whilst the small one is open when the canister is used to purge the RTO.

Figure 1b shows the operational sequence of the three canisters. In particular, the RTO alternates its functioning among three configurations, indicated as A, B and C. The three configurations follow each other in the sequence A-B-C-A-B-C-etc, and it takes 90 s before the switching valves redirect the gas flow from a configuration to the following.

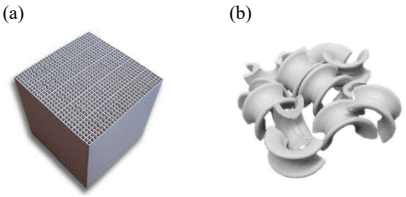

Figure 2. Structured and unstructured ceramic packings inside the canisters: a) monolithic blocks and b) random saddles.

3. Numerical model

A CFD model of the RTO is developed to solve Favre-averaged Navier-Stokes (FANS) and transport/reaction equations for the chemical species. Since the high number of equations and the complex domain make transient simulations too computationally expensive, a steady state approach was adopted. However, to account for the transient behavior of the RTO, a 1-D dynamic model was developed to get information about methane flow rate at the burner as well as axial temperature and heat transfer coefficient profiles along the ceramic media at different instants and configurations.

3.1. 1-D dynamic model

The model assumes just 2 canisters and hence it comprises the inlet monolithic blocks and random packings, the combustion chamber, the outlet random packings and monolithic blocks. The model solves 1-D dynamic conservation equations for energy of both gas and solid phases, as follows:

$$\varepsilon\frac{\partial}{\partial t}(\rho c T)+\frac{\partial}{\partial x}\left(\rho c u T-\varepsilon k\frac{\partial T}{\partial x}\right)=-h a_{gs}(T-T_s) \quad (1)$$

$$(1-\varepsilon)\frac{\partial}{\partial t}(\rho_s c_s T_s)+\frac{\partial}{\partial x}\left(-(1-\varepsilon)k_s\frac{\partial T_s}{\partial x}\right)=h a_{gs}(T-T_s)-q_d \quad (2)$$

where u is the gas superficial velocity. ρ, c and k are the density, specific heat capacity and thermal conductivity of the gas, while ρ_s c_s and k_s are the corresponding properties for the solid. T and T_s are the gas and solid temperatures, respectively, while q_d is heat dissipation through the external surface of the canisters, respectively. The ceramic medium has a void fraction ε and an interfacial area per unit volume a_{gs}.

h represents the heat transfer coefficient which is estimated from correlations for the Nusselt number. More specifically, the Colburn-Chilton analogy is considered for the monolithic blocks having channels with a square cross section of side d:

$$\mathrm{Nu} = \frac{\mathrm{hd}}{\mathrm{k}} = \mathrm{Sh}\left(\frac{\mathrm{Pr}}{\mathrm{Sc}}\right)^{0.33} \quad (3)$$

with,

$$\mathrm{Sh} = 0.766\left(\frac{\mathrm{d}}{\mathrm{L}}\mathrm{ReSc}\right)^{0,483} \quad (4)$$

where L is the length of the monolithic channel and Sh, Sc, Pr and Re are the Sherwood, Schmidt, Prandtl and Reynolds numbers, respectively. For the random saddles, the following correlation for the Nusselt number is used [4]:

$$\mathrm{Nu} = \frac{\mathrm{hd_r}}{\mathrm{k}} = 2 + 1.8\,\mathrm{Re}^{0.5}\mathrm{Pr}^{0.33} \quad (5)$$

where d_r represents the characteristic dimension of the saddles, which can be evaluated as $d_r = 6(1-\varepsilon)/(\varphi a_{gs})$, with φ being the sphericity of the saddles. This is set equal to 0.3 [4].

The global energy balance in the combustion chamber is used to determine the amount of auxiliary fuel, i.e. methane, needed as

$$Q_{CH_4} + Q_{VOC} = Q_d + Q_{heat} \quad (6)$$

where Q_{CH_4} and Q_{VOC} are the thermal power generated from methane and VOC combustion, respectively; Q_d is the dissipated heat and Q_{heat} is the amount of power needed to heat the gas from the inlet to the set point temperature.

The model is implemented in COMSOL Multiphysics (COMSOL, 2018) by using a spatial discretization consisting of 25 elements per bed length and a temporal discretization with a time step < 1 s. Further details on the model and boundary conditions for Eqs. 1-2 are provided in Giuntini et al. A linear temperature profiles for both solid and gas phases is set as initial condition to solve the above equations by using cycles characterised by a switching time t_{sw}= 90s. When the time t approaches t_{sw}, the gas velocity direction is inverted, while swapping the gas inlet and outlet. Calculations are run until a pseudo steady-state is attained, i.e. all cycles are equal.

3.2. 3-D CFD model

FANS equations for continuity, momentum, energy and transport of chemical species in steady state condition are solved using the commercial code Fluent v 19.2 by ANSYS Inc., based on finite volume method. The Reynolds stress tensor is closed with the Realizable k–ε model. The production or consumption of the chemical species due to chemical reactions is modelled by using the Finite Rate/Eddy Dissipation model to handle the turbulence/chemistry interaction. VOCs are represented by benzene and global kinetic schemes are employed for the oxidation reactions of both methane (auxiliary fuel) and benzene. The radiative transfer equation is solved with the P1 model by estimating the spectral properties of the gas medium with the Weighted Sum of Gray Gases model (WSGG) [10].

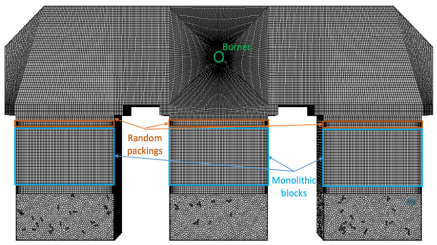

Figure 3. Computational grid.

The computational domain (see Figure 3) comprises porous domains (i.e., for the monolithic blocks and random packings) and fluid domains (i.e., for the combustion chamber, the inlet, outlet, and purge sections). The grid consists of 2.5 million cells and is hybrid, being fully structured in the ceramic media and the combustion chamber, while being made of polyhedrons in the inlet, outlet and purge regions.

Boundary conditions consisted of: uniform velocity, composition and temperature at the RTO and burner inlets; pressure outlet at the exit; no slip condition with negative heat flux at the walls of the combustion chamber. Vertical profiles of heat transfer are set along the random packings and monolithic blocks by using an User Defined Function. These profiles are estimated as

$$Q = ha_{gs}(T_s - T_g) \quad (7)$$

from the profiles of solid temperature T_s and heat transfer coefficient h. T_s and h are provided by the 1-D dynamic model at different instants within the RTO operating cycle and for different RTO configurations (i.e., A, B and C)

A second order upwind interpolation scheme is employed with the SIMPLEC algorithm for pressure-velocity coupling. At convergence normalized residuals did not change with iterations and were all well below 10^{-4}. Besides, physical variables were monitored to confirm convergence.

3. Results

3.1. 1-D dynamic model

Information gained from the 1-D model are shown in Figure 4. Here the axial temperature profiles along the random saddles and the monolithic blocks in the inlet and outlet canister are reported at the initial and final instants of the cycle, which are t = 1 s and t = 90 s, respectively. At the initial time of the cycle, the gas enters the combustion chamber with an higher temperature, of about $T_{in,cc}$ = 1130K, corresponding to the instant when the ceramic masses are hottest; viceversa, at the end of

the cycle, the ceramic masses are cold, hence the gas enters the chamber with a lower temperature, of about $T_{in,cc}$ = 1020 K. For this reason, to keep constant the set-point temperature inside the chamber, a lower flow rate of methane, of about 0.003 m^3/s, is fed at the initial time, increasing to about 0.186 m^3/s at the switching time.

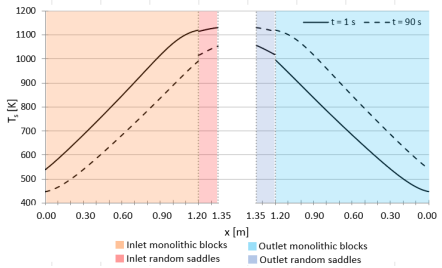

Figure 4. Axial profiles of temperature inside the inlet and outlet ceramic media at t = 1 s and t = 90 s, as predicted by the 1-D dynamic model.

In addition, the temperature of the outgoing gas is lower and of about 450 K at the initial time of the cycle, since the ceramic masses in the outlet canister are colder, while it increases up to 560 K at the end of the cycle. The predicted profile of solid temperature reported in Figure 4, along with the corresponding profiles of heat transfer coefficient, permit to define the axial profiles of heat flux to be set to the porous domains of the CFD model, according to Equation 7, at distinct instants within a cycle, i.e. t = 1 s and t = 90 s, and for different RTO configurations, i.e. A, B and C. In the purge canister, by considering a negligible heat exchange during the switching of the valves, the initial and final temperature profiles are set equal to the final profile (i.e., t = 90 s) of the inlet canister and to the initial profile (i.e., t = 1 s) of the outlet canister, respectively.

3.2. 3-D CFD model

The 3-dimensional CFD simulations were performed for the three different RTO configurations depicted in Figure 1b. The predicted velocity distribution is shown in Figure 5 in the vertical plane, sited at 1/4 of the RTO depth. Figure 5 refers to A configuration, but similar considerations can be drawn for B and C modes. In the inlet region, we can identify a zone with intense turbulence, where the gases strongly recirculate, reaching velocities up to 26 m/s. Such recirculation takes place because the gas enters the RTO with a significant momentum and its passage is obstructed by the presence of the monolithic blocks, which are placed immediately above. After some recirculation, the gas succeeds in passing through the small channels of the monolithic blocks, flowing upwards in the laminar regime; moreover, we can notice that the gas gradually increases its velocity, consistently

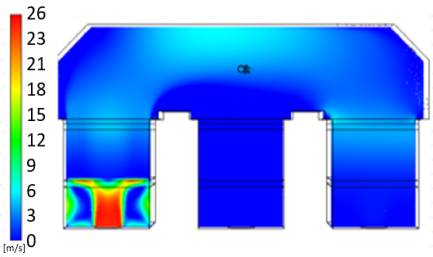

Figure 5: Velocity magnitude distribution in the vertical plane placed at z = ¼ Z at t = 90 s for configuration A.

to the increase in temperature, while it crosses the hot ceramic medium. In the combustion chamber the flow shows a parabolic trajectory with high velocity in the top part of the chamber, reaching velocities up to 7 m/s. After exiting the combustion chamber, the gas crosses the cold ceramic media placed in the outlet canister: here the gas slows down, consistently with its gradual cooling. For the sake of completeness, we must pay attention to the fact that, among the three RTO configurations, only in the A mode the gas crosses the entire combustion chamber, while in the other two configurations (B and C) only a half of the chamber is crossed by the gas, since the inlet and outlet canisters are neighbours.

The predicted pressure field inside the RTO, for configuration A, is depicted in Figure 6. We can notice that the pressure losses are mainly concentrated in the porous domains, i.e. monolithic block and random saddles, of the inlet and outlet canister, while they can be neglected in the combustion chamber and the purge canister. The total pressure drop calculated by the model is of 3000 Pa, consisting of about 1500 Pa in each canister.

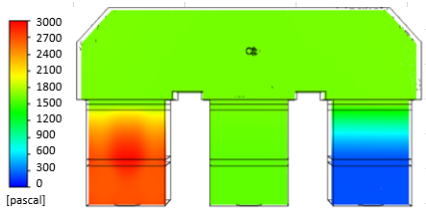

Figure 6: Pressure field predicted by the CFD model at t = 1 s for the configuration A.

To validate the predicted data on pressure drops against experimental data, available in the real plant, also losses through the inlet and outlet valves have to be considered in the model. For this reason, a dedicated model for these regions is developed, as shown in Figure 7.

a)

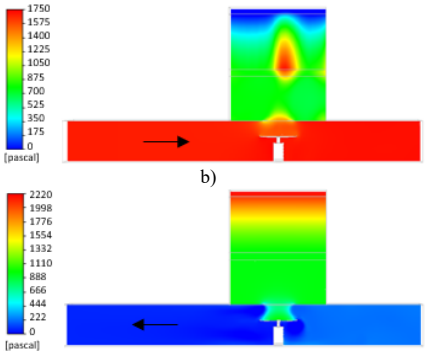

Figure 7: Pressure field predicted by the CFD model in the a) inlet and b) outlet regions of the RTO.

The pressure fields depicted in Figure 7, confirm that a large pressure drop is given by the porous domains; however, the gas experiences a non-negligible pressure drop also crossing the inlet and outlet valves. In addition, we must notice that the losses in the outlet region (2220 Pa) are higher than in the inlet region (1750 Pa); in fact, the outlet stream is hotter, thus it experiences higher velocities, producing higher pressure drops. Figure 8 shows how the sum of the pressure drops (ΔP) across the inlet and outlet regions gives a value of about 4000 Pa, that is in satisfactory agreement with the value of 3800 Pa measured experimentally.

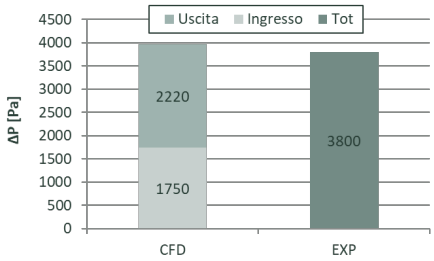

Figure 8: Validation of the CFD model against experimental data on pressure drops.

Figure 9 shows the path-lines coloured by temperature for configuration A, at the initial and final instants of a switching cycle. In addition, we have plotted the iso-surfaces marking the region at temperature above 1173 K as well as the contour of temperature on the random packing of the outlet canister.
At first glance, observing the path-lines, we can notice a strong variation in the gas temperature during the RTO operation; this phenomenon is related to the variation of the solid temperature with time, as predicted by the 1-D dynamic model. Indeed, at t = 1 s, the gas enters the combustion chamber with a higher temperature, than at t = 90 s; for this reason, at the final time of the cycle, the set-point temperature of 1123 K is ensured only in the final region of the chamber, that is after the burner. In addition, the 1173 K iso-surfaces clearly highlight the zones where methane combustion occurs, and these regions appear quite concentrated in the lower part of the chamber. These regions are characterized by very high temperatures, with the flame impinging on the random packing of the outlet canister, as shown by the temperature contours plotted there. These contours show that the gas reach a higher maximum temperature at t = 90 s than at t = 1 s, consequently to the larger flow rate of methane required at the final time, in order to ensure the set-point temperature.

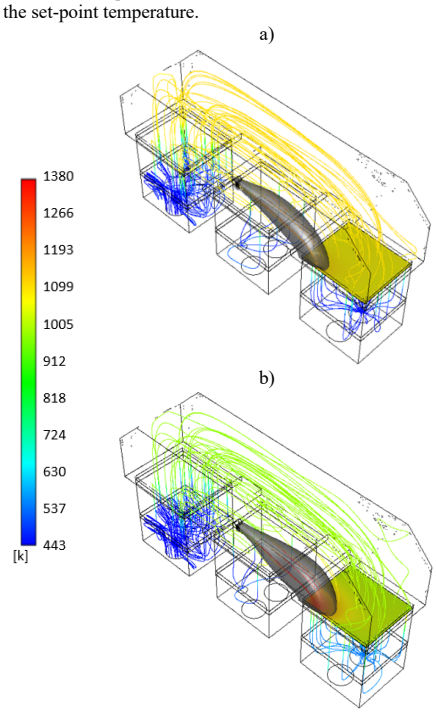

Figure 9: Pathlines coloured by temperature for A configuration at t = 1 s (a) and t = 90 s (b). On each plot is depicted an iso-surface of temperature with T = 1173 K, and a temperature contour on the random packing of the outlet canister.

Figure 10 shows the predicted Destruction and Removal Efficiencies, DREs, in the outlet stream for the three configurations at different instants within the switching cycle. DRE represents the number of molecules of VOCs destroyed, relative to the number of molecules that enter the RTO. We can observe that the highest removal efficiencies are reached in the A mode, which guarantees DRE > 99.995% at all instants, since is the only configuration that allows the gas stream to cross all the combustion chamber. On the other hand, the lowest

efficiencies are achieved in the B mode; in fact, in this configuration the burner is located immediately above the outlet canister, thus the set-point temperature can only be ensured in a very restricted area of the combustion chamber. However, also in this configuration is ensured a DRE > 99.91%. The C configuration presents a behaviour that is intermediate between the A and B ones. It is noteworthy that the DRE is systematically higher at t = 90 s in all the configurations, as a consequence of the higher flow rate of methane required at the end of the switching cycle, in order to guarantee the set-point temperature. Hence, even if at the initial time the combustion chamber is globally hotter, a better VOCs abatement is obtained when very high temperatures are reached, as it happens at t = 90 s. Experimental monitoring of VOCs concentration allowed to calculate an average experimental DRE = 99.2%, that is in good agreement with the model predictions, especially considering the global kinetics employed in the numerical simulations.

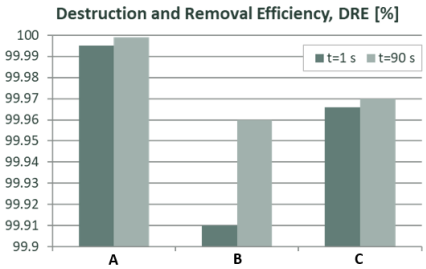

Figure 10: Destruction and Removal Efficiency, DRE [%], for the three configurations A, B and C, at = 1 s and t = 90.

4. Conclusions

An industrial-scale Regenerative Thermal Oxidizer based on a 3-canisters design is analysed through Computational Fluid-Dynamics techniques, by implementing a new methodology to reduce the computational cost of the numerical simulations. To this purpose, a 1-D model, which solves transient energy balances for both solid and gas phases, is coupled to steady-state 3-D CFD simulations. The 1-D model provides information on solid temperature profiles and heat transfer coefficient profiles as well as on methane flow rates at different times within the RTO operation. Then, steady-state CFD simulations are carried out by incorporating the above data for different configurations (i.e., A, B, C) and instants (i.e.,t = 1 s and t = 90 s). In this manner we are able to investigate the fluid-dynamics and the thermo-chemical behaviour of the RTO in time, though avoiding computationally-expensive transient simulations. The model is validated against experimental data on pressure drops and DRE, showing a satisfying agreement. We observe that some configurations are characterized by higher Destruction and Removal efficiencies than others, highlighting the importance of ensuring high temperatures and high residence times inside the combustion chamber. In addition, the analysis of the temperature fields shows the presence of localized hotspots on the random packing of the outlet canister; this is particularly true at the switching time, i.e. t = 90 s, when a large flow rate of methane is fed at the burner, resulting in a large flame which impinges on the ceramic saddles. To this purpose, a proper revision of the burner position should be considered to reduce the thermal aging of the random packing. We believe that the present model provides a useful tool to assist the design and optimization of RTOs.

5. Acknowledgements

This work was supported by the R.T.O. project, POR FESR 2014-2020 Asse 1, funded by Regione Toscana (Italy).

6. References

[1] A.S.K. Warahena et al, Energy recovery efficiency and cost analysis of VOC thermal oxidation pollution control technology, Environmental Science & Technology 43 (2009) 6101–6105.

[2] P. Marín et al., Reverse flow reactors as sustainable devices for performing exothermic reactions: Applications and engineering aspects, Chemical Engineering and Processing - Process Intensification 135 (2019) 175–189.

[3] M. Demichela et al., Risk-based design of a regenerative thermal oxidizer, Industrial & Engineering Chemistry Research 43 (2004) 5838–5845.

[4] M. Amelio et al., Numerical evaluation of the energetic performances of structured and random packed beds in regenerative thermal oxidizers, Applied Thermal Engineering 27 (2007) 762–770. Energy: Production, Distribution and Conservation.

[5] S. Frigerio et al., Improve efficiency of thermal regenerators and VOCs abatement systems: An experimental and modeling study, Experimental Thermal and Fluid Science 31 (2007) 403–411. Fourth Mediterranean Combustion Symposium.

[6] B.-S. Choi et al., Simulation and optimization on the regenerative thermal oxidation of volatile organic compounds, Chemical Engineering Journal 76 (2000) 103–114.

[7] W.J.Y.X. Hao Xiaowen et al., Numerical simulation of a regenerative thermal oxidizer for volatile organic compounds treatment, Environmental Engineering Research 23 (2018) 397–405.

[8] K. Gosiewski et al., Aerodynamic CFD simulations of experimental and industrial thermal flow reversal reactors, Chemical Engineering Journal 373 (2019) 1367–1379.

[9] Giuntini et al., Coupled CFD and 1-D dynamic modeling for the analysis of industrial Regenerative Thermal Oxidizers, Chemical Engineering and Processing - Process Intensification 157 (2020) 108117.

[10] T. F. Smith et al. *J. of Heat Tranf.* 1982.